Supplementary Materials

Animals and MCAO model

Adult male C57BL/6J mice, aged 60-70 days and weighing 20-25g, were bought from the Beijing Vital River Company. All animals were reared in a no pathogenic environment at standard temperature (22–24 °C) with a 12-hour light/dark cycle. The mice were assigned blindly and randomly treated with either MCAO or Sham surgeries. In brief, mice were anesthetized with chloral hydrate (30 mg/kg) intraperitoneally, and the body temperature of which should be kept at 37.0 ± 0.5 °C with incubator throughout the operation. First, the mice were fixed at supine position and the skin was incised along the center of the neckline. Then, the exposed left common carotid artery, external carotid artery and internal carotid artery were ligated separately. A 6-0 silicon rubber-coated monofilament (Doccol, 602256PK5Re) was slowly inserted into the internal carotid artery until the middle cerebral artery was completely obstructed. The left middle cerebral artery was blocked for 60 min to induce transient focal cerebral ischemia. Afterwards, the filament was withdrawn to restore cerebral blood flow (CBF). The laser speckle flowmetry (PeriCam PSI, Stockholm Sweden) was used to monitor the dynamic change of the regional CBF. The successful MCAO model was featured with a cliff-like drop upon insertion of the monofilament and used in subsequent experiments. In the Sham group, mice were treated with the identical surgical process, in which the middle cerebral artery was not occluded. Finally, the mice recovered from the surgery and were kept in the normal condition. All experimental procedures were approved by the Animal Ethics Committee of Tianjin Medical University General Hospital.

Tissue dissociation for 10x Genomics

A total of six male C57BL/6J mice from MCAO and sham groups (three for each group) were used to perform scRNA-seq. After 24 h ischemia-reperfusion, mice were anesthetized, fixed and perfused with ice-cold PBS to remove the blood. The ischemic hemisphere (MCAO ipsilateral brain) and the ipsilateral hemisphere (Sham ipsilateral brain) were immediately dissected and minced using a scalpel for digestion with papain (Worthington, Biochemical Corporation, USA) for 30 minutes at 37°C. The minced brain tissues were triturated gently 4 times with a 10 ml pipette during the incubation process. After incubation, the mixture was centrifuged at 300g for 5 minutes at RT. Then discard the supernatants and resuspend cell pellets in DNase dilute albumin-inhibitor solution. After that, the suspended single cells were passed through a pre-wet (with HBSS) 40 μm cell strainer and centrifuged at 300g for 5 min at 4°C. And then resuspend cell pellets in 10 ml of 30% Percoll in PBS, and which were centrifuged at 700 g for 10 min. After the myelin debris fraction floating on the surface was removed, the pelleted cells were immediately resuspended with FACS buffer (PBS, 1% BSA). Live/dead discrimination reagents for flow cytometry were prepared using Zombie NIR Fixable Viability Kit (BioLegend). BD FACS Aria II sorter was used for FACS sorting. Cells were sorted into the catching medium (0.04% BSA in PBS). The single cell samples were counted by Countess™ II Automated Cell Counter using a hemocytometer with trypan blue. The cell viability was above 80%, and cells were loaded onto a 10x Genomics Chromium chip according to the manufacturer's instructions.

Single cell cDNA library preparation and sequencing

Single Cell 3' Library was constructed mainly following Chromium Single Cell 3' Reagent Kits User Guide (v2 Chemistry). Briefly, the gel bead emulsion (GEM) was generated from the mixture of single cell suspension, gel beads and oils via the 10x Genomics chromium controller. Since droplet formation, samples were added into PCR tubes, and reverse transcription was fulfilled via a T100 Thermal Cycler (Bio-Rad) as follows: incubation at 53℃ for 45 minutes, 85℃ for 5 minutes and then held at 4℃. The cDNA was generated, amplified, and then subjected to quality assessment using an Agilent Bioanalyzer 2100. The library construction was performed by

adding the P5 primer, Read 2 (primer site for sequencing read 2), Sample Index and P7 primer, respectively. The resulting library was quality controlled and then sequenced by Illumina HiSeq4000 PE125.

Quality control analysis of scRNA-seq datasets

The single-cell RNA sequencing data was further analyzed by using the 10x Cell Ranger (version2.2.0, https://support.10xgenomics.com/single-cell-gene-expression/software/pipelines/latest/what-is-cell-ranger).Briefly, FASTQ files were generated by demultiplexing the Illumina sequencer's base call files (BCLs), and then alignment, filtering, barcode and UMI counting were processed. STAR（Spliced Transcripts Alignment to a Reference）was utilized to perform the read alignments to mouse reference transcriptome (mm10). Cell Ranger was employed to conduct primary quality control (QC) on the FASTQ files to generate high quality data. Finally, we recovered 58,528 cells with a median UMI count of 2,610 per cell, a mean read depth of 92,207 reads per cell, and a median of 1,295 genes per cell. Cellranger aggr pipeline was used to combine the data from the sham and MCAO samples for direct comparison and analysis. Seurat is a popular R package that can perform QC following criteria as below: 1)cells were sequenced according to the number of genes from small to large, and select the top 99%; 2)the gene counts > 200; 3)cells with mitochondrial gene expression ratio≤25%.Then, the filtered gene barcode matrices were processed for dimensionality reduction, clustering, and visualization.

Single-cell RNA-seq data analysis

The PCA (principal component analysis) was carried out using the Seurat R Package to identify the first 10 principal components in the feature-barcode matrices for dimensionality reduction. Next, the t-SNE (t-distributed stochastic neighbor embedding), and the UMAP algorithm were used for visualization of the reduced data in two-dimensional space and expression similarity analysis, respectively. The visualization of data was performed by Loupe Cell Browser Software (v3.1.0) and Seurat for clustering, heatmap generation, and differential gene expression analysis.

Differential expression analysis and cell type identification

In order to identify DEGs within each cluster, the Seurat function FindAllMarkers() was employed to find, for each cluster, genes that are more highly expressed in that cluster relative to the rest of the clusters. The Log2 fold-change (L2FC) was used as an estimate of the log2 ratio of mean gene expression in a cluster to that in all other clusters and cells, based on a negative binomial test. The p-value of the output data reported here had been adjusted for multiple testing using the Benjamini-Hochberg procedure. Cell type annotation was identified mainly based on the marker genes from previous studies and the CellMarker database. The sample dates of cells were assigned to marker genes within each cell type for validating the cell type assignments.

Gene enrichment and pathway analysis

The absolute log2FC > 0.5 and P <0.05 were set as a threshold for significantly DEGs. In this study, we conducted the following differential expression comparisons: (1) the DEGs between one cell type and the remaining cell types for identifying cell-type marker genes; (2) the DEGs between MCAO and sham control samples for identifying disease associated changes at the cell type level; (3) the DEGs between one subcluster of a given cell type and the remaining subclusters of the same cell type for determining subcluster specific genes. All these DEGs mentioned above served as input for gene enrichment analysis via Metascape (https://metascape.org), a web-based bioinformatics portal for gene annotation and analysis resource that especially supports meta-analysis of multiple gene lists. To perform gene enrichment analysis, we first identified all statistically enriched terms (GO Biological Processes, KEGG Pathway and Reactome Gene Sets), and calculated accumulative hypergeometric p-values and enrichment factors for filtering. Then, we performed

hierarchical clustering using the significant terms into a tree according to Kappa-statistical similarities among their gene patterns, and the tree was casted into term clusters upon the threshold (0.3 kappa score). Given that Circos plot is a more intuitive and scalable presentation compared to a Venn diagram; we used the former to display the overlap among the gene lists. Different genes were linked in the network if they shared the same ontology term, which was significantly enriched in both input gene lists. To avoid linked genes based on very general annotation, functional overlaps were calculated relying on ontology terms that contain less than 100 genes. For cell-type specific DEGs between MCAO and sham groups, we conducted the enrichment analysis using the online resources Enrichr (http://amp.pharm.mssm.edu/Enrichr/), WebGestalt (http://www.webgestalt.org) and PANTHER (Protein Analysis Through Evolutionary Relationships, http://pantherdb.org).

Single-cell regulatory network inference and clustering (SCENIC) analysis

SCENIC is an algorithm for simultaneously reconstructing gene regulatory networks and identifying stable cell states from single-cell RNA-seq data. Gene regulatory networks were inferred according to co-expression and DNA motif prediction, and then network activity was evaluated in each cell to identify cell status. SCENIC analysis was conducted on each cell type according to the pySCENIC tutorial. SCENIC simultaneously reconstructs gene regulatory networks from single-cell RNA sequencing data. First, SCENIC identifies potential TF targets according to coexpression. TF motif enrichment analysis was then performed to recognize the direct targets (regulons) and assess the activity of the regulons (AUCell score).

Trajectory Analysis

The genes of Mon/Mφ were input for trajectory analysis via the Monocle2 R package (version 2.14.0, https://bioconductor.org/packages/release/bioc/html/monocle.html), and dimensionality reduction was conducted by applying DDRTree method with default parameters. The branch expression analysis modeling (BEAM) implemented in Monocle 2 was employed to identify specific genes that are enriched along particular branches in the pseudotime tree. Branched heatmaps were created with the significant branch-specific expression genes(q value$<5\times10^{-5}$). The orderCells function was analyzed by using the root state argument to specify the homeostatic Mon/Mφ branch as the start point of the trajectory.

Cellular interactions analysis

Molecular interactions between the cells were identified by the recently developed CellPhoneDB. Normalized and filtered scRNA-seq data with the clusters previously identified by Seurat were used for CellPhoneDB analysis. Since the current CellPhoneDB release only accepts human ensembl IDs as input, murine ensembl IDs were converted to human ensembl IDs using biomaRt. The ligand-receptor pair was included in the analysis only when the percentage of cells expressing the receptor and ligand genes exceeded 30%. For the polymeric complexes, the expression value of the subunit with lower average expression was selected as the expression of the receptor for following statistical analysis. Besides, this software could identify the cell type-specific ligand–receptor interactions according to their priority. Then, pair comparisons were performed between all cell types in the data set. First, the cell type markers of all cells were randomly arranged 1000 times to form a new cell cluster, and the average expression level of the ligand in the randomly arranged cell cluster and the average expression level of the receptor in the interacting cell clusters were calculated. Finally, a zero distribution is generated for each ligand-receptor pair in each pair comparison between the two clusters. The actual mean value of the ligand-receptor pair between the two clusters was calculated, and the likely significant P value of the receptor-ligand pair in the two clusters was estimated according to the proportion of the calculated mean equal to or higher than the actual mean value.

Immunofluorescence Staining

The rodent brain was removed and fixed in 4% PFA overnight. The brain sections were permeabilized with 0.3% Triton X-100 for 10 min, and then washed and blocked with 3% BSA (bovine serum albumin) for 1h at RT. Then the tissue sections were incubated with the primary antibodies including goat anti-Iba-1 (1:800, Abcam),rabbit anti-TMEM119(1:300,Abcam), mouse anti-CXCL10 (1:50, Abcam), mouse anti-APC(1:100, Millipore), rabbit anti-GPD1(1:500, Biorbyt), goat anti-CD72(1:100, R&D Systems), rat anti-CCL11(1:100, R&D Systems), goat anti-CD13(1:20, R&D Systems),Armenian Hamster anti-CCL2(1:100, eBioscience), rat anti-LGALS3(1:100, eBioscience), FITC-linked rabbit anti-LILRB4(1:100, MyBioSource), Alexa Fluor® 594 anti-CD8a (1:150, Biolegned), rabbit anti-Iba-1 (1:1000,Wako), goat anti-OPN(1:20, R&D Systems), mouse anti-EP4 (C-4)(1:250, Santa Cruz Biotechnology) at 4ºC overnight. After primary incubation, the brain sections were washed with cold PBS, and then incubated with the secondary fluorescent-conjugated antibodies: Alexa Fluor 546-conjugated donkey anti-mouse, Alexa Fluor 546-conjugated donkey anti-goat, Alexa Fluor 546-conjugated donkey anti-rabbit, Alexa Fluor 546-conjugated goat anti-rat, Alexa Fluor 647-conjugated donkey anti-rabbit, Alexa Fluor 647-conjugated donkey anti-goat, Alexa Fluor 594-conjugated donkey anti-mouse, Alexa Fluor 488-conjugated goat anti-Armenian Hamster, Alexa Fluor 488-conjugated donkey anti-rabbit, Alexa Fluor 488-conjugated donkey anti-goat(1:1000, Invitrogen) at room temperature for 1 h. The sections were then washed with PBS and applied coverslip with DAPI - Aqueous, Fluoroshield(104139, Abcam). Immunostaining was observed with EVOS FL Auto Imaging System (Thermo Fisher Scientific),Mantra System (PerkinElmer) and LSM 900 with Airyscan 2(ZEISS).

Flow Cytometry Staining

Brain single cell suspensions were prepared as described above. Aliquot up to 1×10^6 cells/100 μL into FACS tubes. Block Fc receptors by pre-incubating cells with TruStain FcX™ (anti-mouse CD16/32) antibody (Biolegned) for 10 minutes on ice. Add appropriately conjugated fluorescent, or purified primary antibodies at proper concentrations and incubate at 4℃ for 25 minutes in the dark. Then, washed cells with PBS twice. For intracellular staining, cells were fixed in fixation buffer in the dark for 20 minutes at RT after cell surface antigen staining. After washing twice in Intracellular Staining Perm Wash Buffer, cells were incubated with antibodies in the residual Intracellular Staining Perm Wash Buffer for 20 minutes in the dark at RT. Then, cells were washed twice with Intracellular Staining Perm Wash Buffer and centrifuge at 350 g for 5 minutes. Finally, the fixed and intracellularly labeled cells were resuspended in 500 uL PBS and analyzed with the FMO controls to identify gating boundaries. The antibodies used were as following list: (CD45, CD11b, CD31, CD85k (gp49 Receptor), MCP-1, Ly6C, Ly6G, I-A/I-E, Biolegned), (CD13, CD72, BD Biosciences), (Neun, IP10, Abcam), (CD177, O4, CCL11, R&D Systems), (EAAT1/GLAST/SLC1A3, Novus Biologicals), (GPD1, Origene), (IFITM1, GRO beta, PAE Receptor, Biorbyt). Data were obtained from FACSAria III (BD Biosciences), and analyzed using FlowJo 10.

Statistical analysis

All statistical analysis was described in the figure legends and data are presented as mean±SD. Shapiro-Wilk test was applied for the evaluation of normality for each set of data compared. The two-tailed unpaired Student's t-test was used for comparations between two groups. $P < 0.05$ were usually considered to be statistical significance. All statistical analyses were performed using GraphPad Prism 8.0 software.

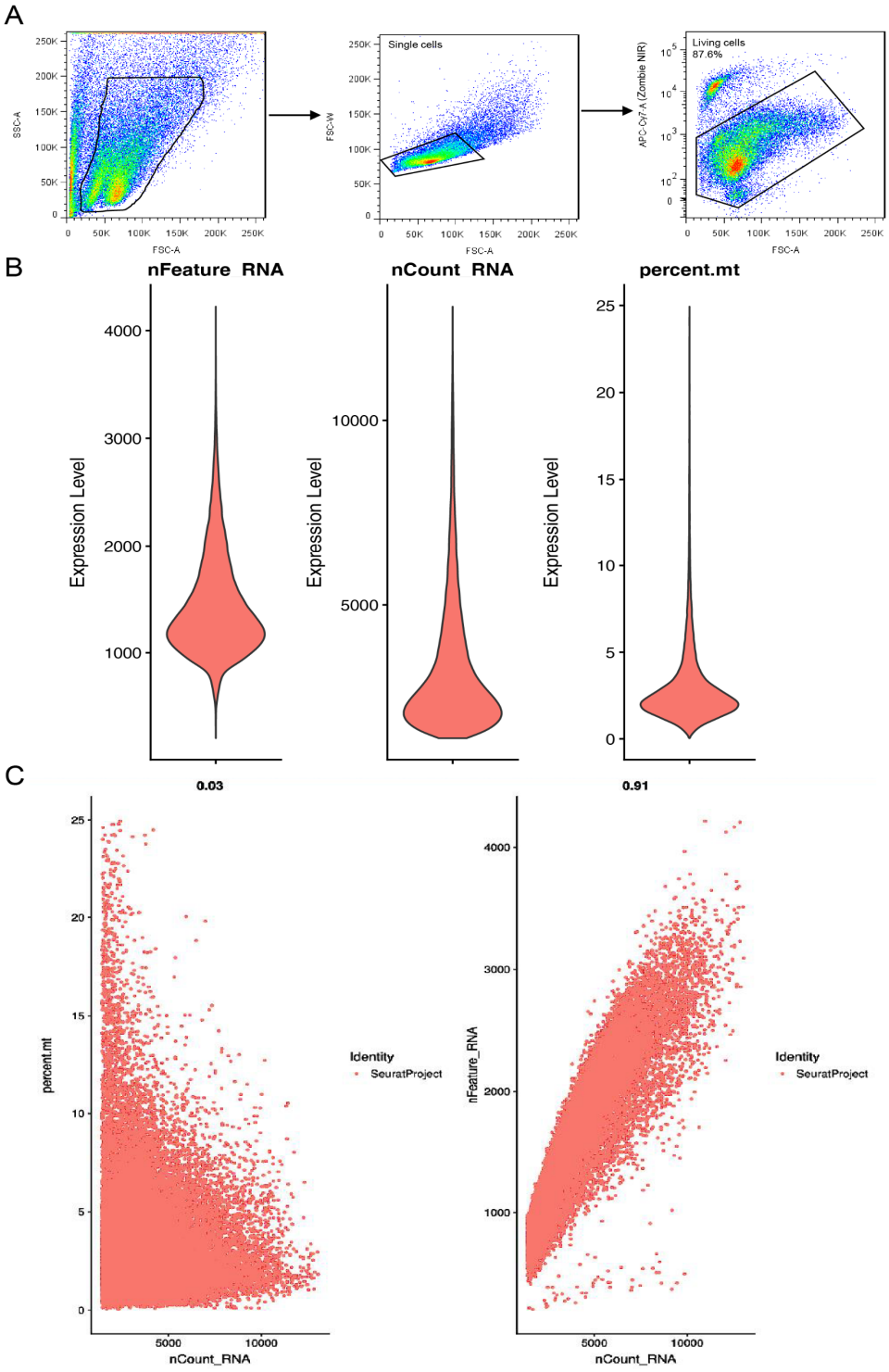

Fig. S1. Quality controls for single cell RNA sequencing. (A)FACS gating strategy for the sorting of living and single cells. **(B)**Number of genes per cell, unique molecular identifier (UMI) counts for single cells and percentage of mitochondrial genes. **(C)** The percentage of mitochondrial genes/all UMI counts per cell and the relation between the total number of genes per cell and UMI counts.

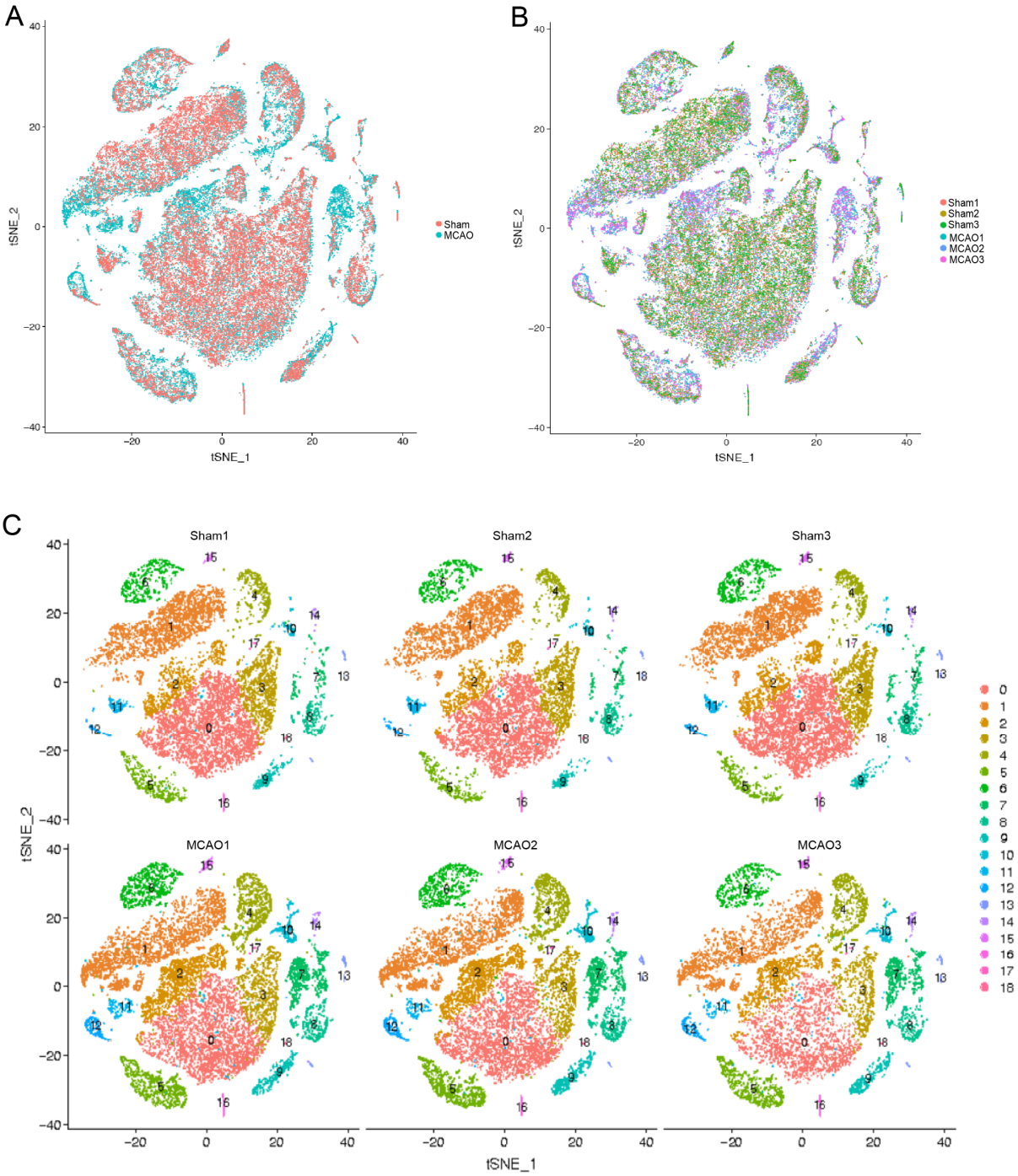

Fig. S2. Clustering of brain cells of Sham and MCAO Mouse Model. (A-C) t-SNE plot showing the distribution of 58,528 cells in a merged dataset from the disease groups**(A)**, merged samples **(B)** and separated samples **(C).**

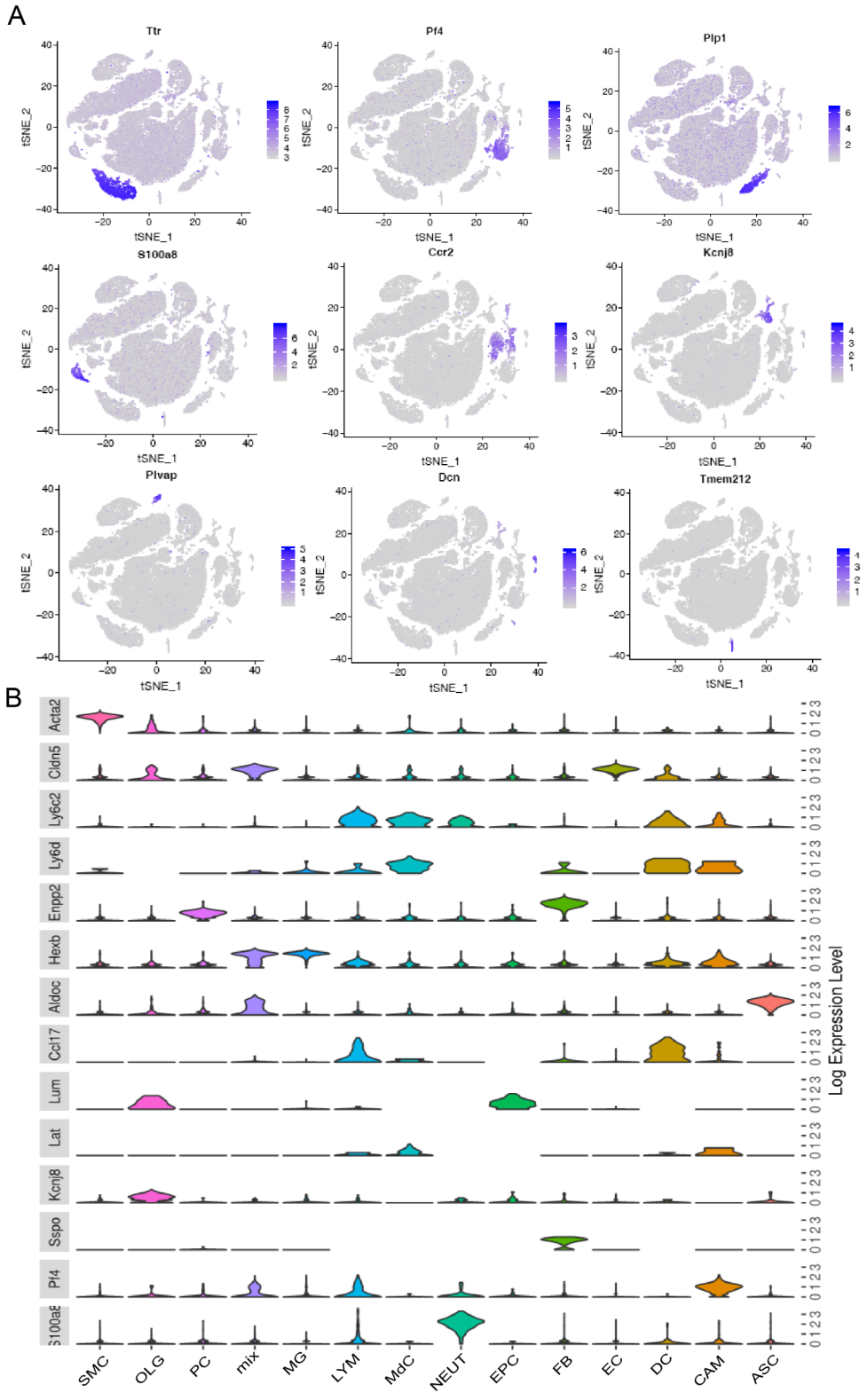

Fig. S3. Classification among cell clusters with marker genes. (A)t-SNE plots showing expression patterns of marker genes in various clusters in aligned data on single cells extracted from the brains of MCAO and Sham mice 24 hours after ischemia reperfusion. Scale in Log expression. **(B)** Violin plots showing the expression of top cell-type specific marker genes in each cluster. Cells were collected from mice in Sham and MCAO groups (three mice for each group).

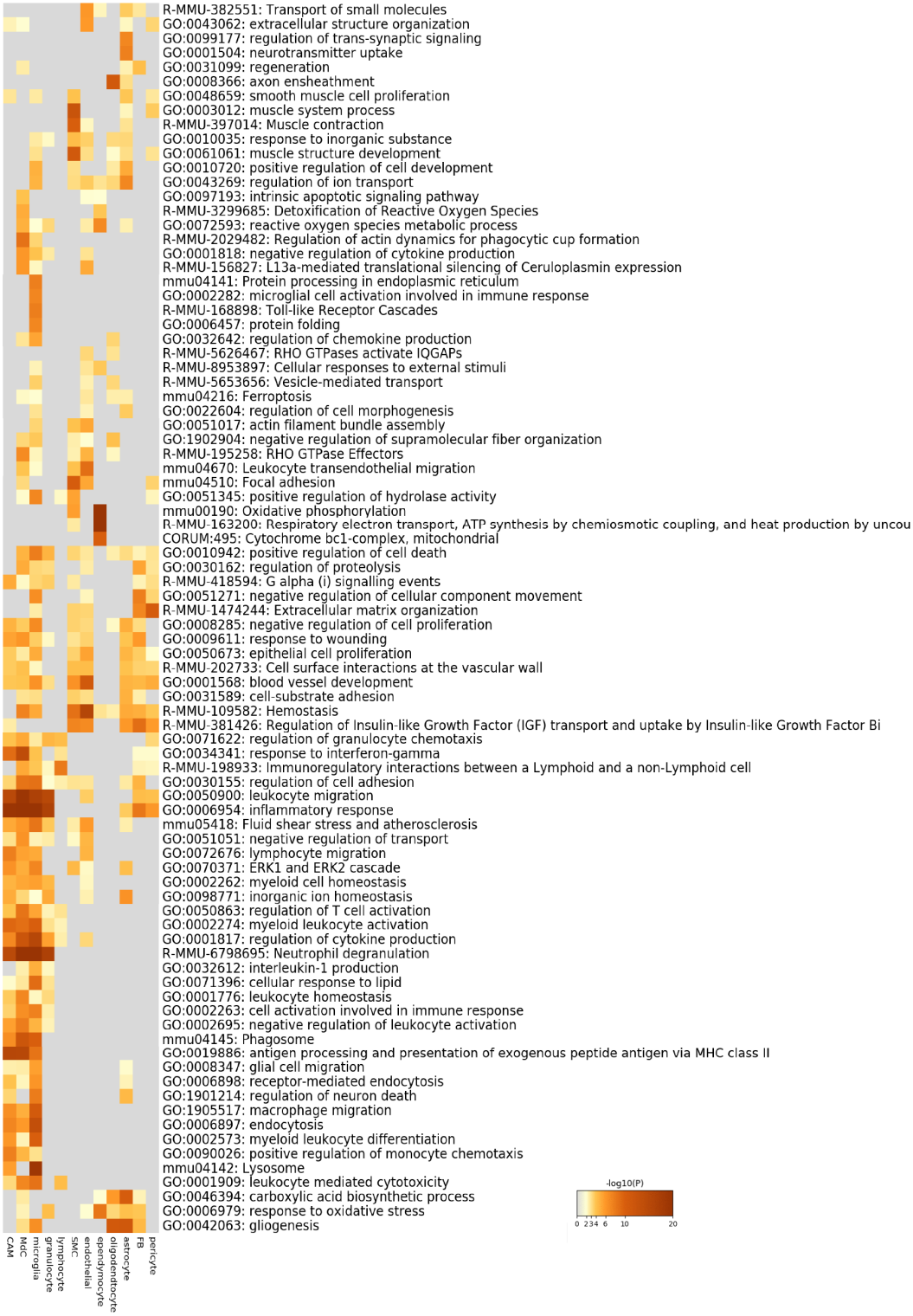

Fig. S4. Heatmap showing the top enriched terms of marker genes for each cell type. The discrete color scale indicates statistical significance. The color key from gray to brown represents high to low P-value, respectively. Gray color indicates a lack of significance.

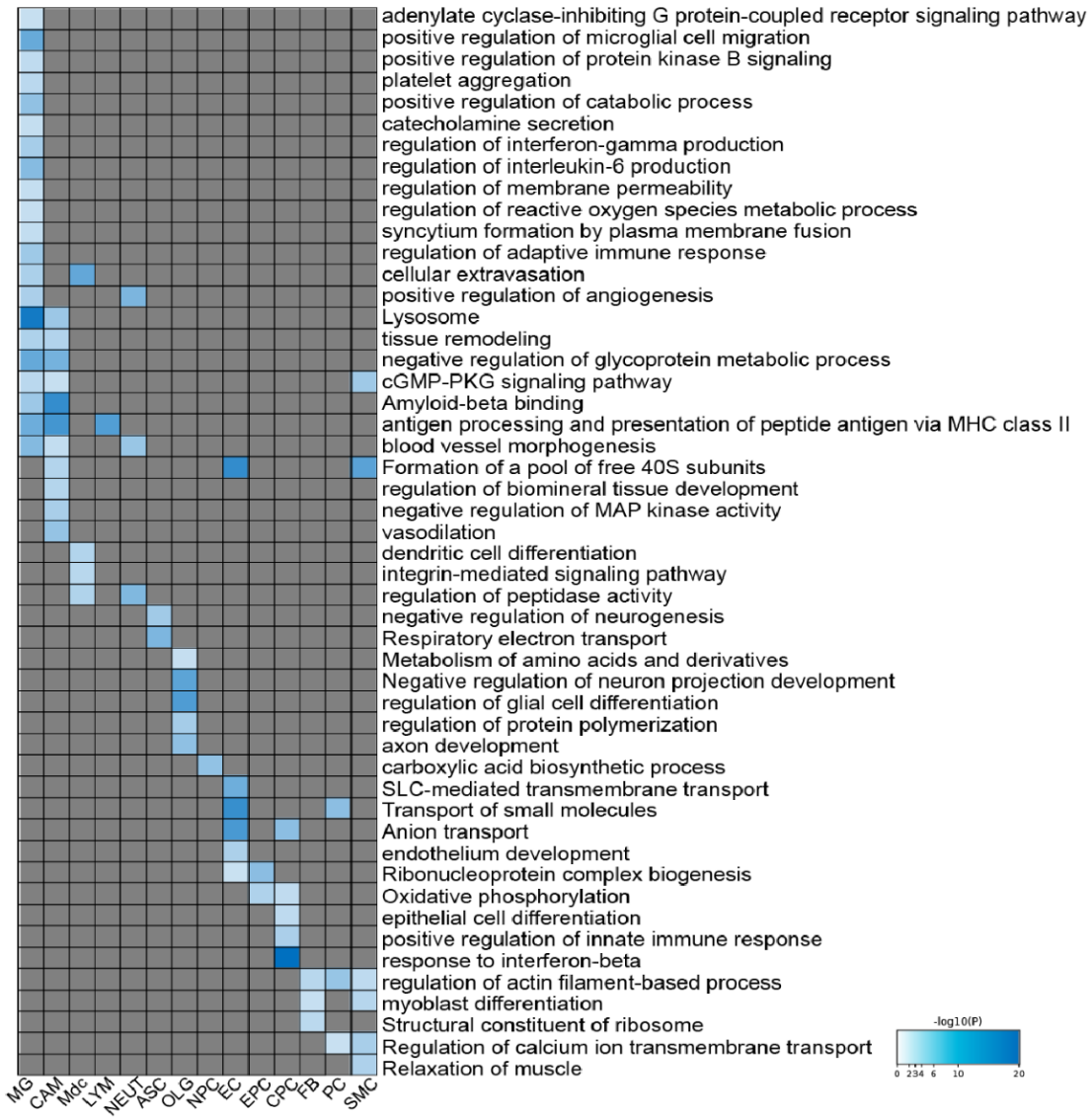

Fig. S5. The pathway and biological process analyses between MCAO and sham group for each cell type cluster. Blue color indicates downregulation. Gray indicates no significant change.

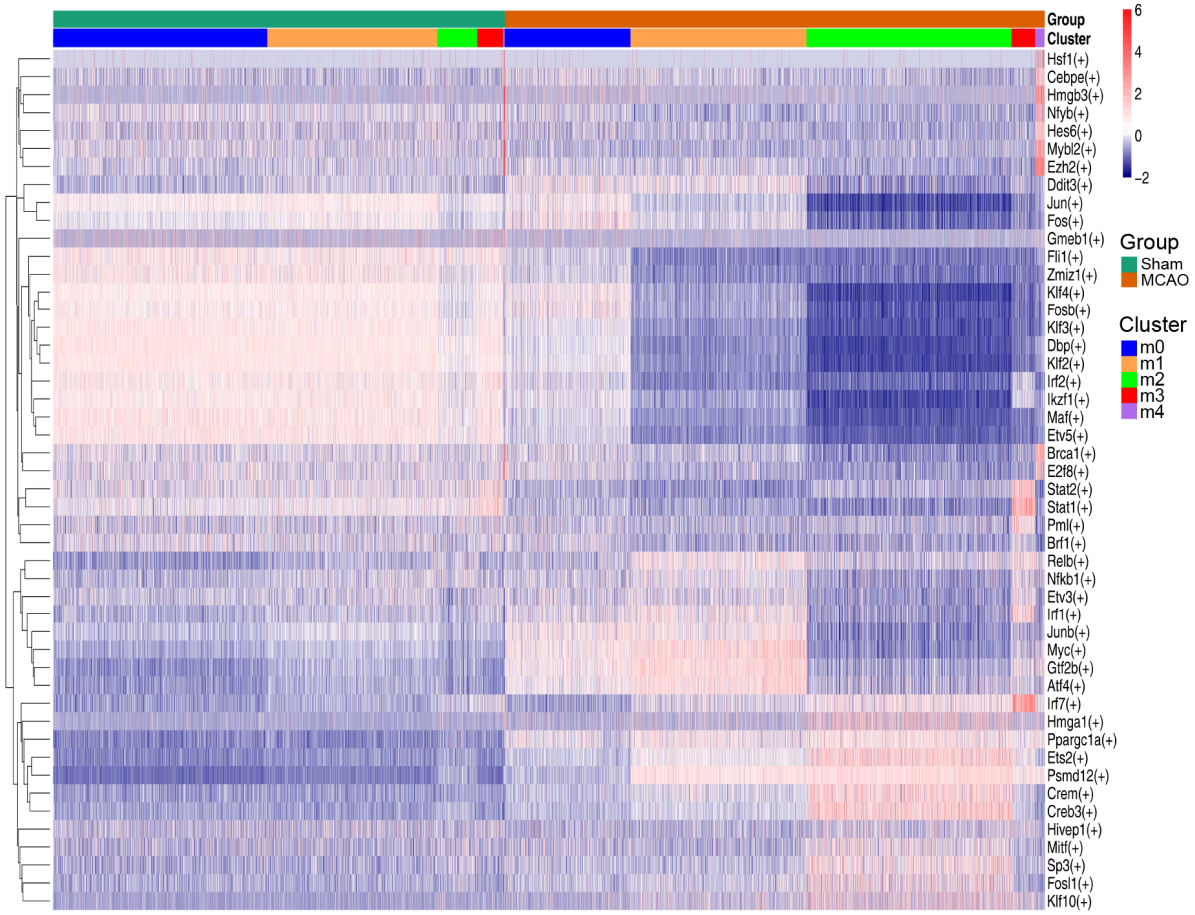

Fig. S6. Heatmap of the average area under the curve (AUC) scores for the expression of genes regulated by TFs (transcription factors), as measured in SCENIC, in five microglia subclusters. The top 10 TFs between subclusters in expression regulation estimates was shown.

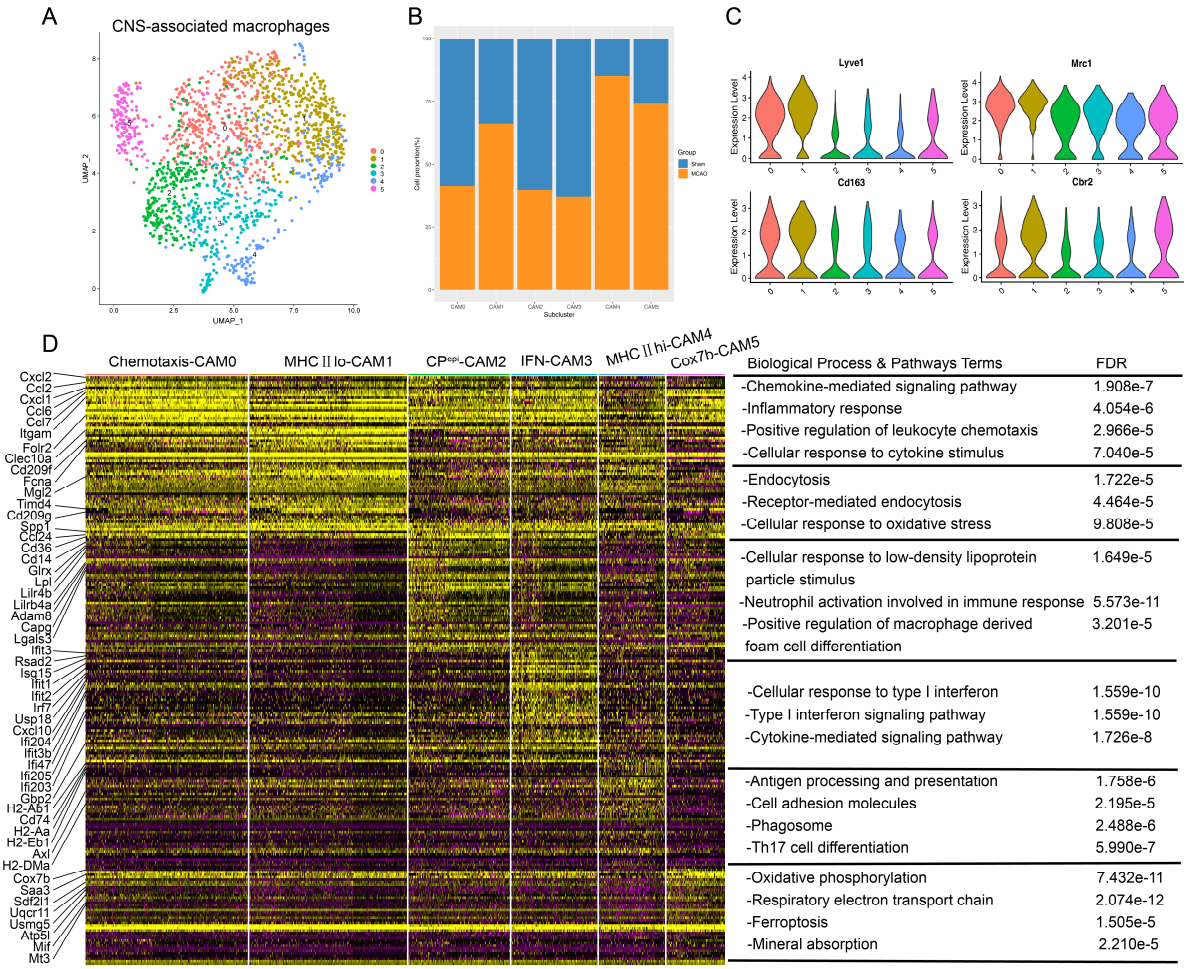

Biological Process & Pathways Terms	FDR
-Chemokine-mediated signaling pathway	1.908e-7
-Inflammatory response	4.054e-6
-Positive regulation of leukocyte chemotaxis	2.966e-5
-Cellular response to cytokine stimulus	7.040e-5
-Endocytosis	1.722e-5
-Receptor-mediated endocytosis	4.464e-5
-Cellular response to oxidative stress	9.808e-5
-Cellular response to low-density lipoprotein particle stimulus	1.649e-5
-Neutrophil activation involved in immune response	5.573e-11
-Positive regulation of macrophage derived foam cell differentiation	3.201e-5
-Cellular response to type I interferon	1.559e-10
-Type I interferon signaling pathway	1.559e-10
-Cytokine-mediated signaling pathway	1.726e-8
-Antigen processing and presentation	1.758e-6
-Cell adhesion molecules	2.195e-5
-Phagosome	2.488e-6
-Th17 cell differentiation	5.990e-7
-Oxidative phosphorylation	7.432e-11
-Respiratory electron transport chain	2.074e-12
-Ferroptosis	1.505e-5
-Mineral absorption	2.210e-5

Fig. S7. The ischemic injury-associated changes in CNS-associated macrophages. (A) UMAP of CNS-associated macrophages (CAMs) isolated from the sham and MCAO at 24h after reperfusion clustering analysis. **(B)** The percentage change tendency of each CAMs cluster during the progression of MCAO. **(C)** Violin plot showing the expression levels of known core signature genes for each subtype of CAMs. **(D)** Heatmap of differentially expressed genes between CAMs populations with representative significant GO Biological Process and Pathway terms.

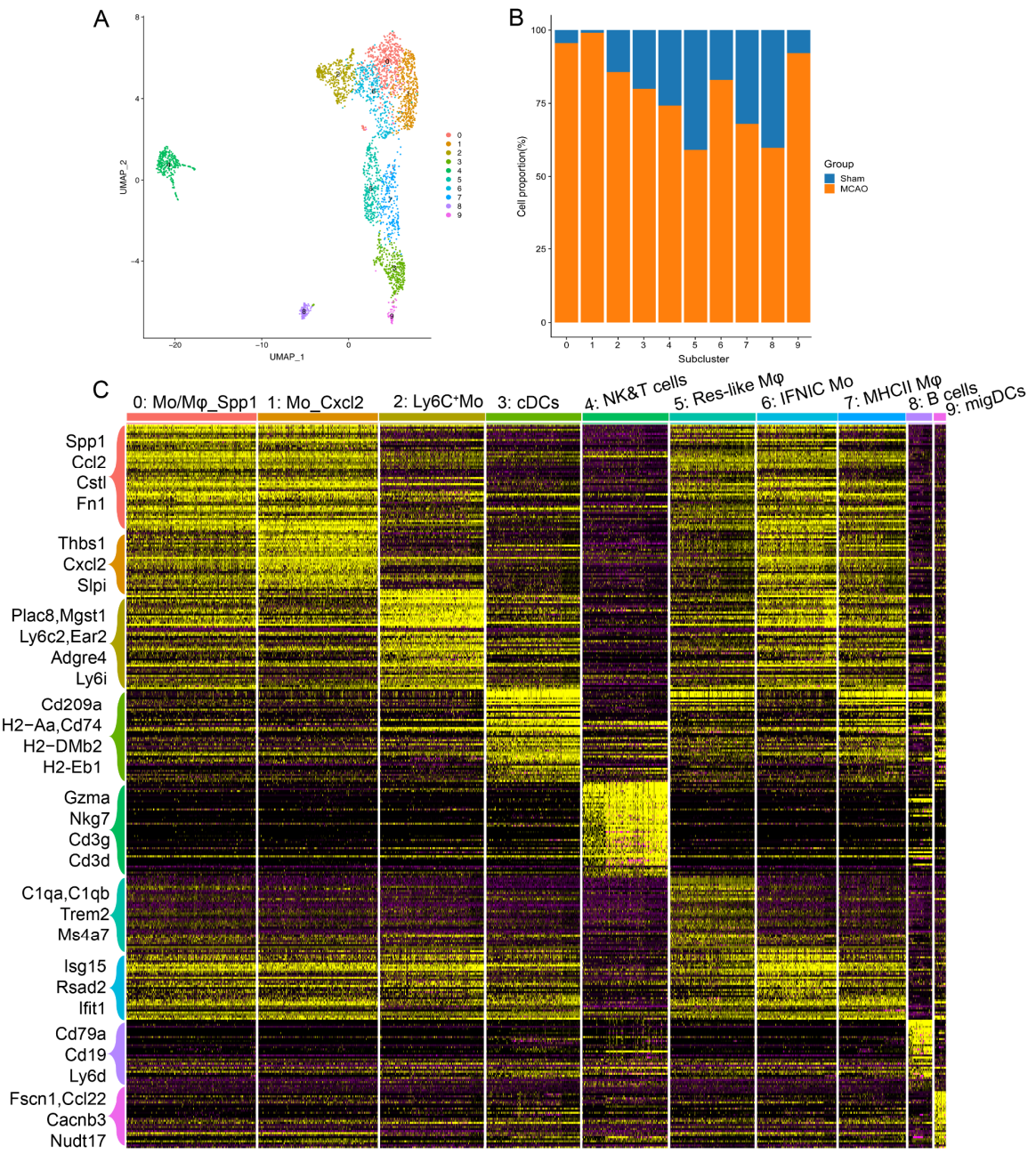

Fig. S8. Differential gene expression patterns in main circulating immune cells clusters. (A) UMAP visualization of subclusters of the main immune cells including monocytes/macrophages, DCs, lymphocytes. **(B)** The bar graph showing the fraction of the main immune cells subclusters originating from disease state. **(C)** Heatmap showing single-cell gene expression of the main immune cells subcluster-specific genes.

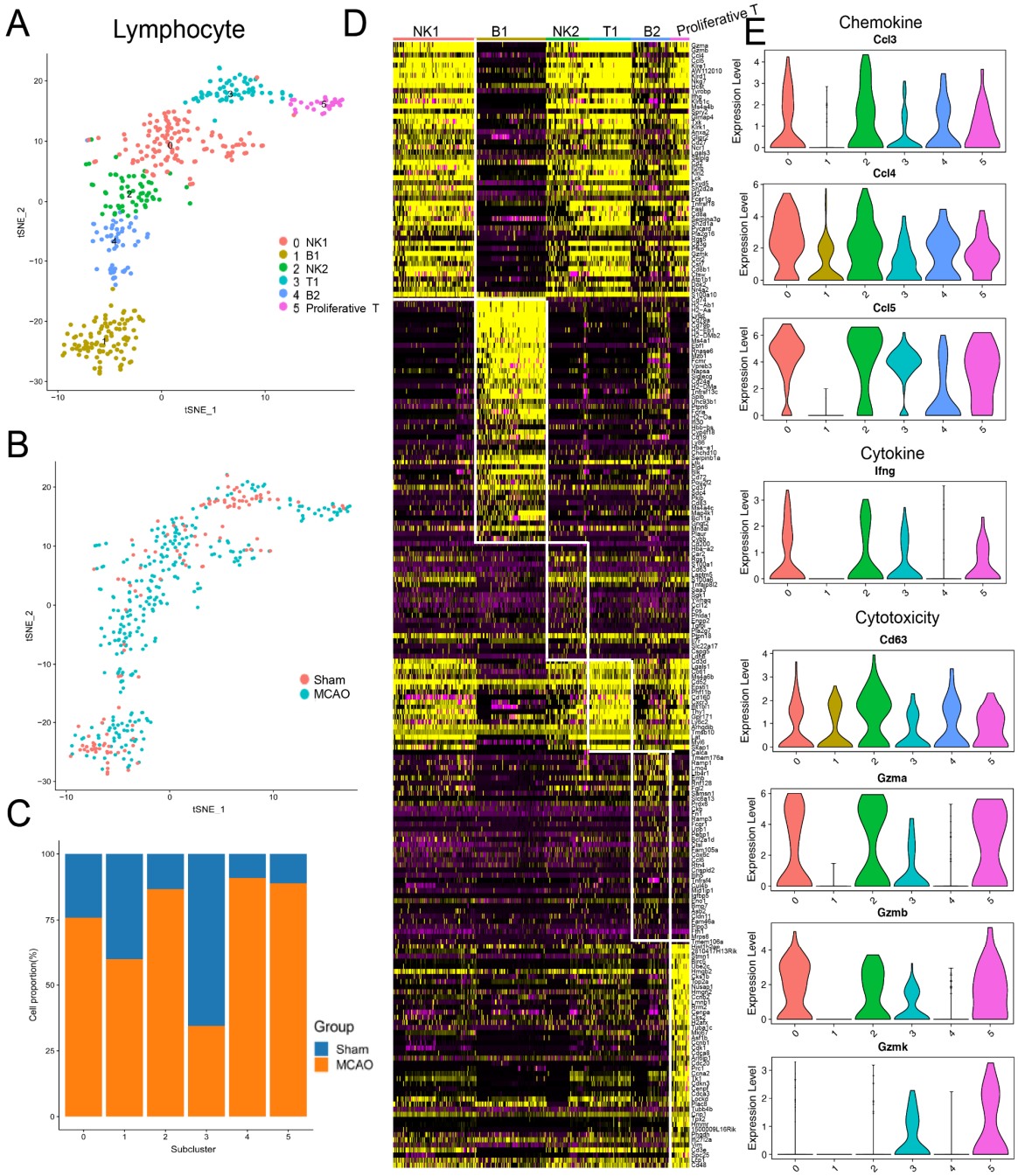

Fig. S9. Lymphocytes sub-clustering analysis upon ischemic injury.

(A, B) t-SNE plots showing the distribution of each subtype of lymphocytes**(A)** and the disease origin of each individual cell**(B)**. **(C)**Bar graphs representing proportion of lymphocytes subtypes within each disease group. **(D)**Heatmap representing gene expression characteristics of the subtypes of lymphocytes **(E)** Violin plots of genes encoding chemokine production, cytokine production and cytotoxicity in lymphocytes subsets.

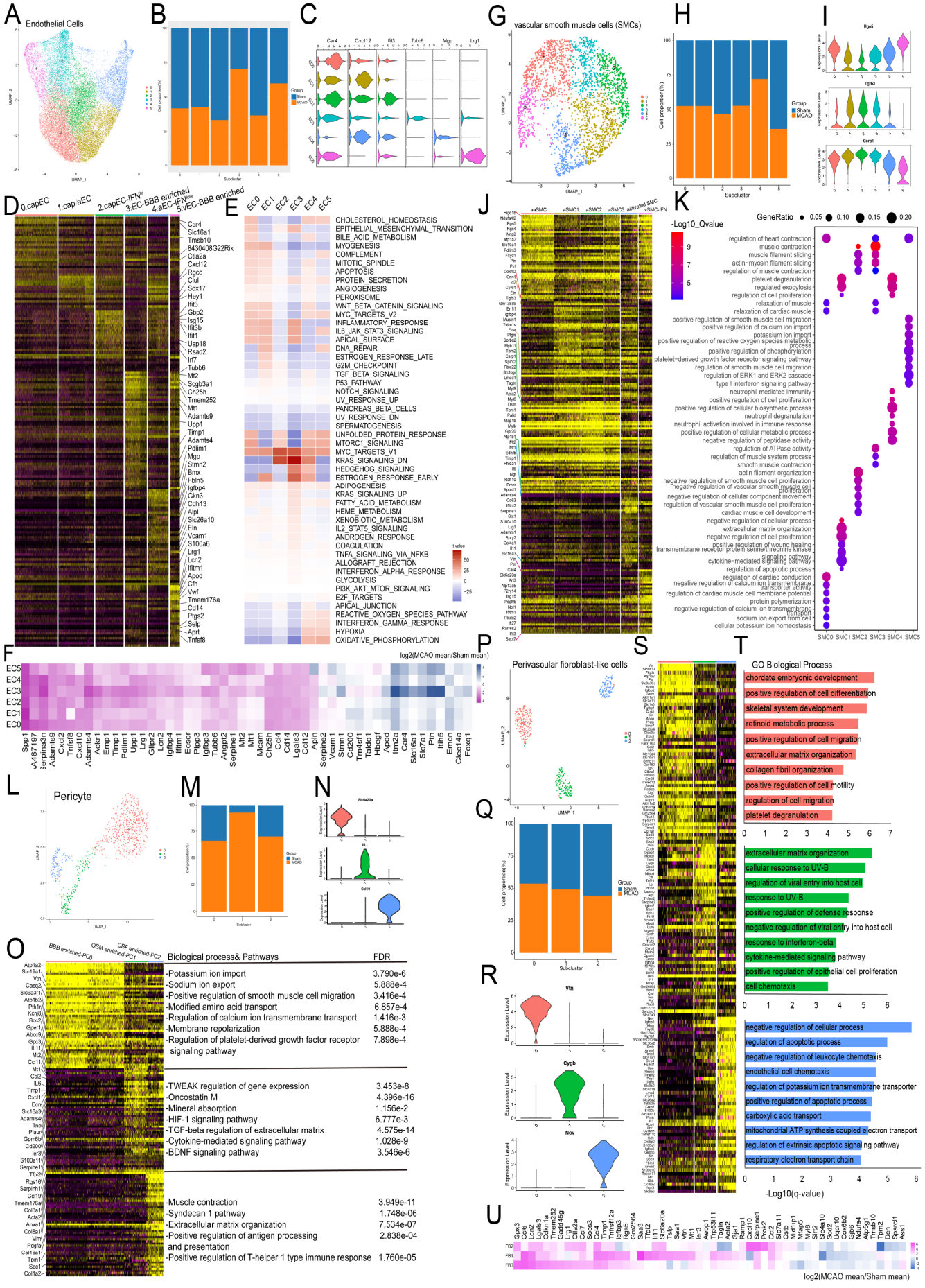
A
Endothelial Cells
B
C
G
vascular smooth muscle cells (SMCs)
H
I
D
0:capEC
1:capAEC
2:capEC-IFN^hi
3:EC-BBB enriched
4:aEC-IFN^low
5:vEC-BBB enriched
E
EC0
EC1
EC2
EC3
EC4
EC5
CHOLESTEROL_HOMEOSTASIS
EPITHELIAL_MESENCHYMAL_TRANSITION
BILE_ACID_METABOLISM
MYOGENESIS
COMPLEMENT
MITOTIC_SPINDLE
APOPTOSIS
PROTEIN_SECRETION
ANGIOGENESIS
PEROXISOME
WNT_BETA_CATENIN_SIGNALING
MYC_TARGETS_V2
INFLAMMATORY_RESPONSE
IL6_JAK_STAT3_SIGNALING
APICAL_SURFACE
DNA_REPAIR
ESTROGEN_RESPONSE_LATE
G2M_CHECKPOINT
TGF_BETA_SIGNALING
P53_PATHWAY
NOTCH_SIGNALING
UV_RESPONSE_UP
PANCREAS_BETA_CELLS
UV_RESPONSE_DN
SPERMATOGENESIS
UNFOLDED_PROTEIN_RESPONSE
MTORC1_SIGNALING
MYC_TARGETS_V1
KRAS_SIGNALING_DN
HEDGEHOG_SIGNALING
ESTROGEN_RESPONSE_EARLY
ADIPOGENESIS
KRAS_SIGNALING_UP
FATTY_ACID_METABOLISM
HEME_METABOLISM
XENOBIOTIC_METABOLISM
IL2_STAT5_SIGNALING
ANDROGEN_RESPONSE
COAGULATION
TNFA_SIGNALING_VIA_NFKB
ALLOGRAFT_REJECTION
INTERFERON_ALPHA_RESPONSE
GLYCOLYSIS
PI3K_AKT_MTOR_SIGNALING
E2F_TARGETS
APICAL_JUNCTION
REACTIVE_OXYGEN_SPECIES_PATHWAY
INTERFERON_GAMMA_RESPONSE
HYPOXIA
OXIDATIVE_PHOSPHORYLATION
J
aaSMC
aSMC1
aSMC2
aSMC3
activated SMC
vSMC-IFN
K
GeneRatio
-Log10_Qvalue
regulation of heart contraction
muscle contraction
muscle filament sliding
actin−myosin filament sliding
regulation of muscle contraction
platelet degranulation
regulated exocytosis
regulation of cell proliferation
relaxation of muscle
relaxation of cardiac muscle
positive regulation of smooth muscle cell migration
positive regulation of calcium ion import
potassium ion import
positive regulation of reactive oxygen species metabolic process
positive regulation of phosphorylation
platelet-derived growth factor receptor signaling pathway
regulation of smooth muscle cell migration
regulation of ERK1 and ERK2 cascade
type I interferon signaling pathway
neutrophil mediated immunity
positive regulation of cell proliferation
positive regulation of cellular biosynthetic process
neutrophil degranulation
neutrophil activation involved in immune response
positive regulation of cellular metabolic process
negative regulation of peptidase activity
regulation of ATPase activity
regulation of muscle system process
smooth muscle contraction
actin filament organization
negative regulation of smooth muscle cell proliferation
negative regulation of vascular smooth muscle cell proliferation
negative regulation of cellular component movement
regulation of vascular smooth muscle cell proliferation
cardiac muscle cell development
negative regulation of cellular process
extracellular matrix organization
negative regulation of cell proliferation
positive regulation of wound healing
transmembrane receptor protein serine/threonine kinase signaling pathway
cytokine-mediated signaling pathway
regulation of apoptotic process
regulation of cardiac conduction
negative regulation of calcium ion transmembrane transporter activity
regulation of cardiac muscle cell membrane potential
protein polymerization
negative regulation of calcium ion transmembrane transport
sodium ion export from cell
cellular potassium ion homeostasis
SMC0
SMC1
SMC2
SMC3
SMC4
SMC5
F
log2(MCAO mean/Sham mean)
EC5
EC4
EC3
EC2
EC1
EC0
P
Perivascular fibroblast-like cells
S
T
GO Biological Process
chordate embryonic development
positive regulation of cell differentiation
skeletal system development
retinoid metabolic process
positive regulation of cell migration
extracellular matrix organization
collagen fibril organization
positive regulation of cell motility
regulation of cell migration
platelet degranulation
extracellular matrix organization
cellular response to UV-B
regulation of viral entry into host cell
response to UV-B
positive regulation of defense response
negative regulation of viral entry into host cell
response to interferon-beta
cytokine-mediated signaling pathway
positive regulation of epithelial cell proliferation
cell chemotaxis
negative regulation of cellular process
regulation of apoptotic process
negative regulation of leukocyte chemotaxis
endothelial cell chemotaxis
regulation of potassium ion transmembrane transporter
positive regulation of apoptotic process
carboxylic acid transport
mitochondrial ATP synthesis coupled electron transport
regulation of extrinsic apoptotic signaling pathway
respiratory electron transport chain
-Log10(q-value)
L
Pericyte
M
N
Q
R
Vtn
Cygb
Nov
O
BBB enriched-PC0
OSM enriched-PC1
CBF enriched-PC2
Biological process& Pathways
FDR
-Potassium ion import 3.790e-6
-Sodium ion export 5.888e-4
-Positive regulation of smooth muscle cell migration 3.416e-4
-Modified amino acid transport 6.857e-4
-Regulation of calcium ion transmembrane transport 1.416e-3
-Membrane repolarization 5.888e-4
-Regulation of platelet-derived growth factor receptor signaling pathway 7.898e-4
-TWEAK regulation of gene expression 3.453e-8
-Oncostatin M 4.396e-16
-Mineral absorption 1.156e-2
-HIF-1 signaling pathway 6.777e-3
-TGF-beta regulation of extracellular matrix 4.575e-14
-Cytokine-mediated signaling pathway 1.028e-9
-BDNF signaling pathway 3.546e-6
-Muscle contraction 3.949e-11
-Syndecan 1 pathway 1.748e-06
-Extracellular matrix organization 7.534e-07
-Positive regulation of antigen processing and presentation 2.838e-04
-Positive regulation of T-helper 1 type immune response 1.760e-05
U
FB2
FB1
FB0
log2(MCAO mean/Sham mean)

Fig. S10. Gene expression alterations in the sub-clustering of vasculature lineage cells after stroke. (A, G, L, P) UMAP representation of endothelial cells (ECs)**(A)**, vascular mural cells (smooth muscle cells (SMCs)**(G)** and pericytes (PCs)**(L)**) and perivascular fibroblast-like cells (FBs)**(P)**. **(B, H, M, Q)** Bar graphs representing proportion of each ECs**(B)**, SMCs**(H)**, PCs**(M)** and FBs**(Q)** subsets within each disease group. **(C, I, N, R)** Violin plot of the representative marker genes in each ECs**(C)**, SMCs**(I)**, PCs**(N)** and FBs**(R)** subsets. **(D, J, O, S)** Heatmap representing gene expression characteristics of the subtypes of ECs**(D)**, SMCs**(J)**, PCs **(O,** left panel**)** and FBs**(S)**. **(E)** GSVA analysis in pathway activities among different ECs subclusters. **(K, O, T)** Gene Ontology analysis based on DEGs of each SMCs **(K)**, PCs **(O,** right panel**)** and FBs**(T)**subclusters. Representative GO terms with Benjamini–Hochberg-corrected P<0.05 (one-sided Fisher's exact test) are displayed. **(F, U)** Heatmap showing the log 2FC in gene expression of the selected ECs **(F)** and FBs **(U)** subcluster-based DEGs between sham and MCAO group.

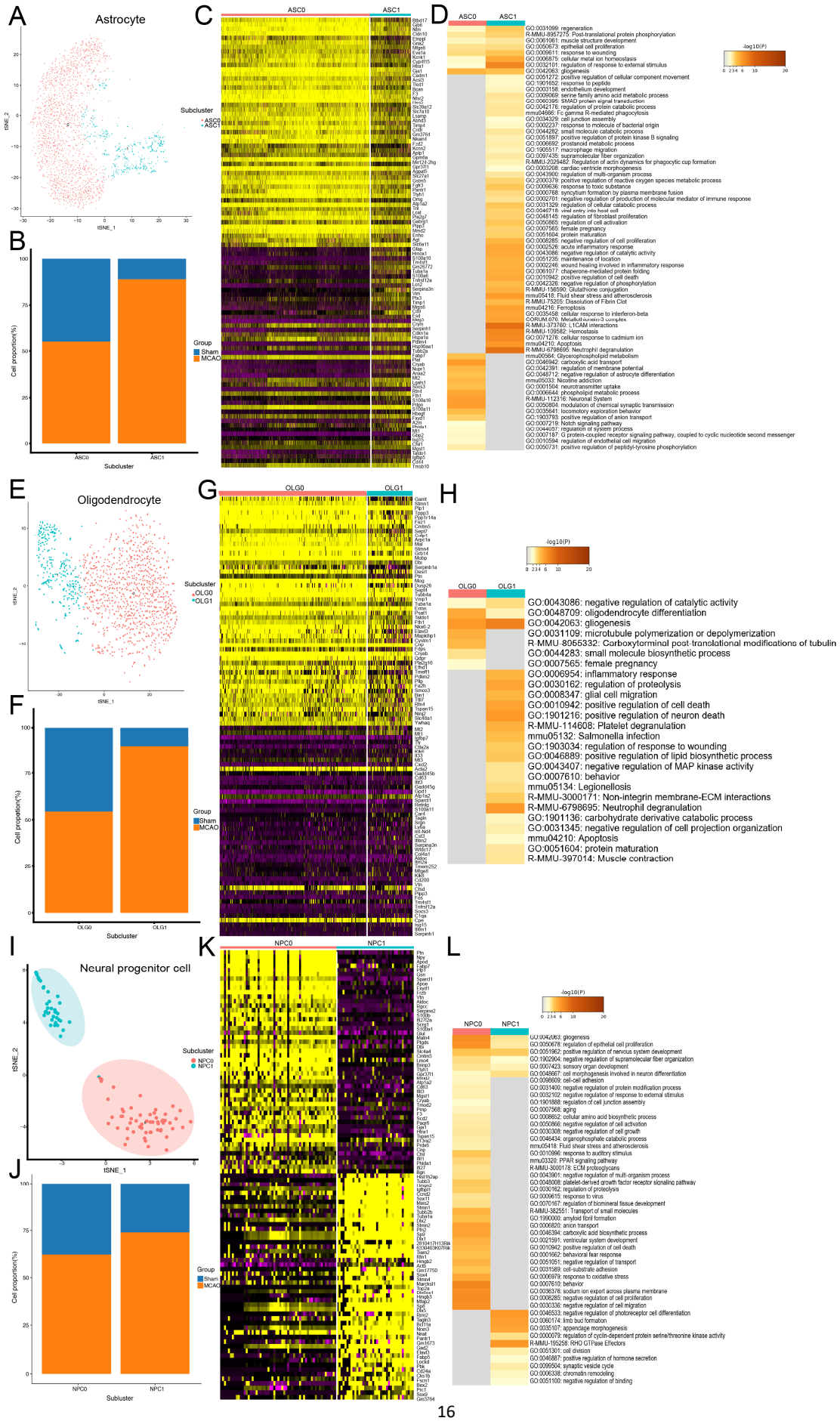
A
Astrocyte
Subcluster
ASC0
ASC1
tSNE_1
tSNE_2
B
Cell proportion(%)
Group
Sham
MCAO
Subcluster
C
ASC0
ASC1
D
ASC0
ASC1
-log10(P)
GO:0031099: regeneration
R-MMU-8957275: Post-translational protein phosphorylation
GO:0061061: muscle structure development
GO:0050673: epithelial cell proliferation
GO:0009611: response to wounding
GO:0006875: cellular metal ion homeostasis
GO:0032101: regulation of response to external stimulus
GO:0042063: gliogenesis
GO:0051272: positive regulation of cellular component movement
GO:1901652: response to peptide
GO:0003158: endothelium development
GO:0009069: serine family amino acid metabolic process
GO:0060395: SMAD protein signal transduction
GO:0042176: regulation of protein catabolic process
mmu04666: Fc gamma R-mediated phagocytosis
GO:0034329: cell junction assembly
GO:0002237: response to molecule of bacterial origin
GO:0044282: small molecule catabolic process
GO:0051897: positive regulation of protein kinase B signaling
GO:0006692: prostanoid metabolic process
GO:1905517: macrophage migration
GO:0097435: supramolecular fiber organization
R-MMU-2029482: Regulation of actin dynamics for phagocytic cup formation
GO:0003208: cardiac ventricle morphogenesis
GO:0043900: regulation of multi-organism process
GO:2000379: positive regulation of reactive oxygen species metabolic process
GO:0009636: response to toxic substance
GO:0000768: syncytium formation by plasma membrane fusion
GO:0002701: negative regulation of production of molecular mediator of immune response
GO:0031329: regulation of cellular catabolic process
GO:0046718: viral entry into host cell
GO:0048145: regulation of fibroblast proliferation
GO:0050865: regulation of cell activation
GO:0007565: female pregnancy
GO:0051604: protein maturation
GO:0008285: negative regulation of cell proliferation
GO:0002526: acute inflammatory response
GO:0043086: negative regulation of catalytic activity
GO:0051235: maintenance of location
GO:0002246: wound healing involved in inflammatory response
GO:0061077: chaperone-mediated protein folding
GO:0010942: positive regulation of cell death
GO:0042326: negative regulation of phosphorylation
R-MMU-156590: Glutathione conjugation
mmu05418: Fluid shear stress and atherosclerosis
R-MMU-75205: Dissolution of Fibrin Clot
mmu04216: Ferroptosis
GO:0035458: cellular response to interferon-beta
CORUM.070: Metalloproteinase-3 complex
R-MMU-373760: L1CAM interactions
R-MMU-109582: Hemostasis
GO:0071276: cellular response to cadmium ion
mmu04210: Apoptosis
R-MMU-6798695: Neutrophil degranulation
mmu00564: Glycerophospholipid metabolism
GO:0046942: carboxylic acid transport
GO:0042391: regulation of membrane potential
GO:0048712: negative regulation of astrocyte differentiation
mmu05033: Nicotine addiction
GO:0001504: neurotransmitter uptake
GO:1006644: phospholipid metabolic process
R-MMU-112316: Neuronal System
GO:0050804: modulation of chemical synaptic transmission
GO:0035641: locomotory exploration behavior
GO:1903793: positive regulation of anion transport
GO:0007219: Notch signaling pathway
GO:0044057: regulation of system process
GO:0007187: G protein-coupled receptor signaling pathway, coupled to cyclic nucleotide second messenger
GO:0010594: regulation of endothelial cell migration
GO:0050731: positive regulation of peptidyl-tyrosine phosphorylation
E
Oligodendrocyte
Subcluster
OLG0
OLG1
tSNE_1
tSNE_2
F
Cell proportion(%)
Group
Sham
MCAO
Subcluster
G
OLG0
OLG1
H
-log10(P)
OLG0
OLG1
GO:0043086: negative regulation of catalytic activity
GO:0048709: oligodendrocyte differentiation
GO:0042063: gliogenesis
GO:0031109: microtubule polymerization or depolymerization
R-MMU-8955332: Carboxyterminal post-translational modifications of tubulin
GO:0044283: small molecule biosynthetic process
GO:0007565: female pregnancy
GO:0006954: inflammatory response
GO:0030162: regulation of proteolysis
GO:0008347: glial cell migration
GO:0010942: positive regulation of cell death
GO:1901216: positive regulation of neuron death
R-MMU-114608: Platelet degranulation
mmu05132: Salmonella infection
GO:1903034: regulation of response to wounding
GO:0046889: positive regulation of lipid biosynthetic process
GO:0043407: negative regulation of MAP kinase activity
GO:0007610: behavior
mmu05134: Legionellosis
R-MMU-3000171: Non-integrin membrane-ECM interactions
R-MMU-6798695: Neutrophil degranulation
GO:1901136: carbohydrate derivative catabolic process
GO:0031345: negative regulation of cell projection organization
mmu04210: Apoptosis
GO:0051604: protein maturation
R-MMU-397014: Muscle contraction
I
Neural progenitor cell
Subcluster
NPC0
NPC1
tSNE_1
tSNE_2
J
Cell proportion(%)
Group
Sham
MCAO
Subcluster
K
NPC0
NPC1
L
-log10(P)
NPC0
NPC1
GO:0042063: gliogenesis
GO:0050678: regulation of epithelial cell proliferation
GO:0051962: positive regulation of nervous system development
GO:1902904: negative regulation of supramolecular fiber organization
GO:0007423: sensory organ development
GO:0048667: cell morphogenesis involved in neuron differentiation
GO:0098609: cell-cell adhesion
GO:0031400: negative regulation of protein modification process
GO:0032102: negative regulation of response to external stimulus
GO:1901888: regulation of cell junction assembly
GO:0007568: aging
GO:0006652: cellular amino acid biosynthetic process
GO:0030866: negative regulation of cell activation
GO:0030308: negative regulation of cell growth
GO:0046434: organophosphate catabolic process
mmu05418: Fluid shear stress and atherosclerosis
GO:0010996: response to auditory stimulus
mmu03320: PPAR signaling pathway
R-MMU-3000178: ECM proteoglycans
GO:0043901: negative regulation of multi-organism process
GO:0048008: platelet-derived growth factor receptor signaling pathway
GO:0030162: regulation of proteolysis
GO:0009615: response to virus
GO:0070167: regulation of biomineral tissue development
R-MMU-382551: Transport of small molecules
GO:1990000: amyloid fibril formation
GO:0006820: anion transport
GO:0046394: carboxylic acid biosynthetic process
GO:0021591: ventricular system development
GO:0010942: positive regulation of cell death
GO:0001662: behavioral fear response
GO:0051051: negative regulation of transport
GO:0031589: cell-substrate adhesion
GO:0006979: response to oxidative stress
GO:0007610: behavior
GO:0036376: sodium ion export across plasma membrane
GO:0008285: negative regulation of cell proliferation
GO:0030336: negative regulation of cell migration
GO:0046533: negative regulation of photoreceptor cell differentiation
GO:0060174: limb bud formation
GO:0035107: appendage morphogenesis
GO:0000079: regulation of cyclin-dependent protein serine/threonine kinase activity
R-MMU-195258: RHO GTPase Effectors
GO:0051301: cell division
GO:0046887: positive regulation of hormone secretion
GO:0099504: synaptic vesicle cycle
GO:0006338: chromatin remodeling
GO:0051100: negative regulation of binding

Fig. S11. Differential gene expression patterns in other glia lineage cells and stem cells clusters. (A, E, I) t-SNE projection of the astrocytes**(A)**, oligodendrocytes**(E)** and neural progenitor cells**(I)** sub-clustering. **(B, F, J)** Bar graphs representing proportion of each ASCs**(B)**, OLGs**(F)** and NPCs**(J)** subclusters within each disease group. **(C, G, K)** Heatmap representing gene expression characteristics of the subtypes of ASCs**(C)**, OLGs**(G)** and NPCs**(K)**. **(D, H, L)** Gene Ontology analysis of DEGs for each of the ASCs**(D)**, OLGs **(H)** and NPCs**(L)**subclusters. Representative GO terms with Benjamini–Hochberg-corrected P<0.05 (one-sided Fisher's exact test) are displayed.

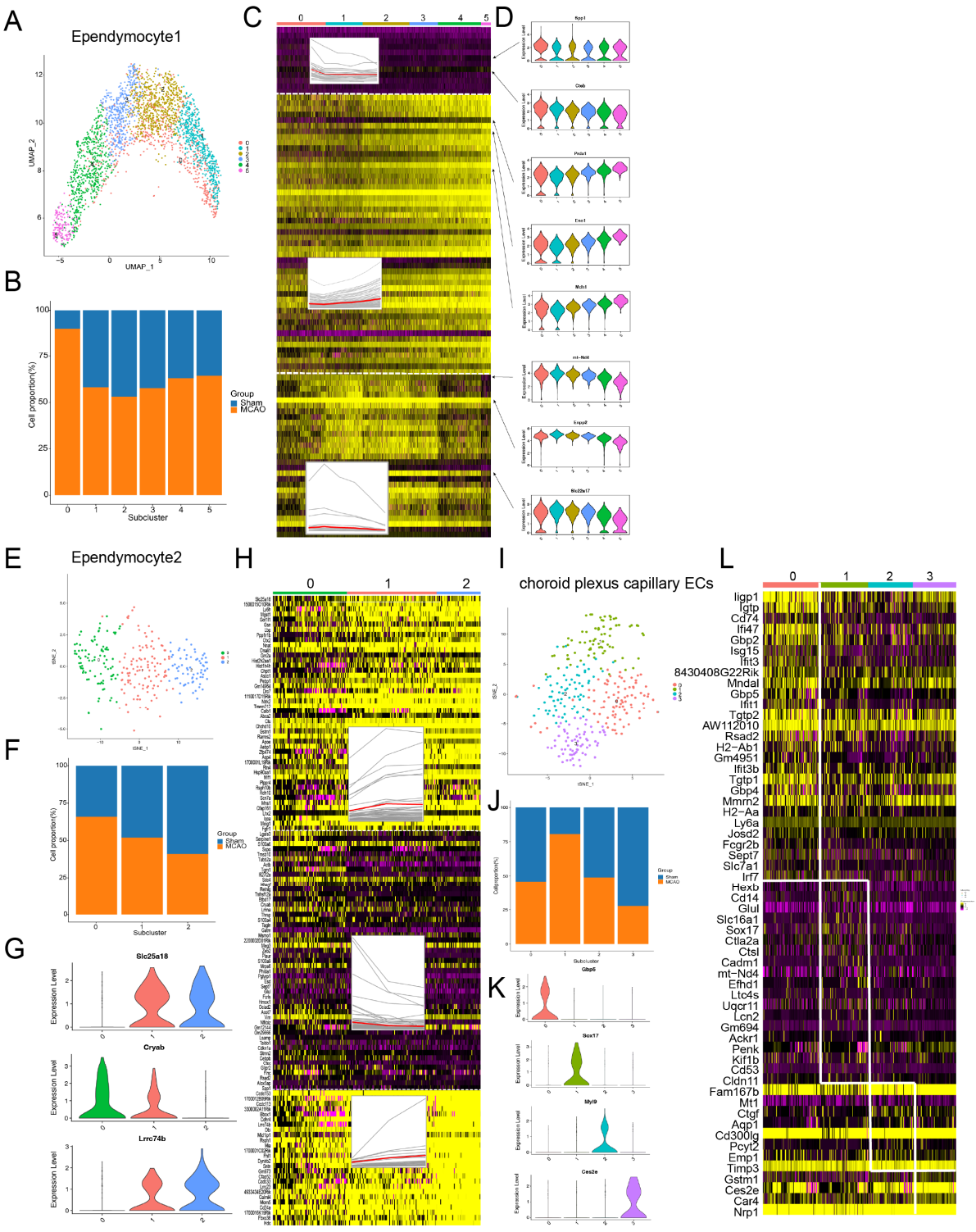

Fig. S12. Gene expression alterations in choroid plexus endothelial cells and ependymal clusters after stroke. (A) UMAP visualization of subclusters of secretory ependymal cells (EPC1). **(E, I)** t-SNE projection of the EPC2**(E)** and choroid plexus capillary ECs (CPCs) **(I)** sub-clustering. **(B, F, J)** Bar graphs representing proportion of each EPC1**(B)**, EPC2**(F)** and CPCs **(J)** subtypes within each disease group. **(D, G, K)** Violin plot of the representative marker genes in each EPC1**(D)**, EPC2**(G)** and CPCs**(K)** subtypes. **(C, H, L)** Heatmap representing gene expression characteristics of the subtypes of EPC1**(C)**, EPC2**(H)** and CPCs**(L)**.

Table S1. Sequencing parameters for cells isolated from the sham and MCAO groups.

	Sham1	Sham2	Sham3	MCAO1	MCAO2	MCAO3
Estimated number of cells	8771	8540	9980	11772	11361	8104
Mean Reads per Cell	107345	130357	121192	93621	90953	149331
Median Genes per Cell	1231	1257	1281	1396	1365	1554
Valid Barcodes	94.9%	94.9%	95.5%	96.2%	96.1%	95.4%
Sequencing Saturation	94.1%	94.9%	94.7%	91.8%	91.9%	93.3%
Q30 Bases in Barcode	96.4%	96.4%	96.2%	96.8%	96.8%	96.8%
Q30 Bases in RNA Read	90.5%	90.5%	89.8%	91.0%	91.4%	92.0%
Q30 Bases in UMI	96.0%	96.0%	95.9%	96.5%	96.5%	96.5%
Reads Mapped Confidently to Genome	90.9%	91.8%	92.1%	92.2%	92.8%	90.0%
Reads Mapped Confidently to Intergenic Regions	4.3%	4.1%	3.9%	3.4%	3.3%	5.3%
Reads Mapped Confidently to Intronic Regions	19.3%	18.5%	18.4%	16.4%	16.1%	17.3%
Reads Mapped Confidently to Exonic Regions	67.3%	69.2%	69.7%	72.4%	73.4%	67.3%
Reads Mapped Confidently to Transcriptome	63.5%	65.3%	65.7%	68.6%	69.6%	63.6%
Reads Mapped Antisense to Gene	1.5%	1.5%	1.5%	1.7%	1.6%	1.5%

Table S2. Top enriched pathways and process among DEGs between MCAO and sham groups of major cell types (P<0.05) and representative DEGs involved in the pathways and process.

Cell type	No. DEGs	Top representative pathways and process	Top representative DEGs
Microglia	275	Neutrophil chemotaxis/Apoptosis Lysosome/Positive regulation of microglia cell migration	Up: Spp1,Lilrb4a,Cd72,Ccl7,Ccl12 Down: P2ry12,Siglech,Gpr34,Selplg,Hpgd
Astrocyte	34	Cellular responses to stress/Signal Transduction Respiratory electron transport	Up: Ccl4,Cdkn1a,Gfap,AY036118,Vim Down: Dbp, Gria2, Ntm, Itm2a, Appl2
Endothelial cell	101	Cellular response to chemical stimulus/Regulation of cell death Anion transport/Transport of small molecules	Up: Ctla2a, Plat, Lrg1, Lcn2, Tmem252 Down: Rps27rt, Cxcl12, Spock2, Ifit3, Itm2a
Oligodendrocyte	80	Cytokine-mediated signaling pathway/Regulation of neuron apoptotic process Regulation of glial cell differentiation/ Negative regulation of neuron projection development	Up: Serpina3n, Tma16, Gpd1, Phactr3, Klk6 Down: Hebp1,1700047M11Rik, Lpar1, Omg, Hs3st1
Ependymocyte	35	Response to steroid hormone/ Regulation of ion transport Oxidative phosphorylation/Ribonucleoprotein complex biogenesis	Up: Spp1,Ccl4,Ccl12,AY036118,Mt2 Down: Defb11,Hist2h2aa1,Usp50,Ifi27l2a, Sostdc1
Pericyte	26	Regulation of secretion/Response to peptide Transport of small molecules	Up: Ednrb,Il11,Timp1,Saa3,Ccl11 Down: Dbp,Itm2a,Cxcl12,Pltp,Tsc22d1
SMC	59	Cellular response to chemical stimulus/Cytokine-mediated signaling pathway Regulation of calcium ion transmembrane transport/Relaxation of muscle	Up: Ifitm1,Ccl4,Cdkn1a,Sdc4,Rasl11a Down: Fbxl22,Pln,Lbh,Crim1,Myh11
CAM	135	Toll-like receptor cascades/Chemokine receptor binding Vasodilation /Amyloid-beta binding	Up: Arg1,Saa3,Cxcl2,Msr1,Ccl6 Down: Hist4h4,Hpgd,Maf,Lst1,Clec10a
Neutrophil	67	Neutrophil degranulation/IL-1 signaling pathway	Up: Cxcl3,Ccrl2,Cxcl2,Marcksl1,Hcar2

		regulation of peptidase activity	Down: Ltf,Camp,Cd177,Ngp,Ly6g
MdC	153	Myeloid leukocyte migration/Acute-phase response Cellular extravasation/Integrin-mediated signaling pathway	Up: Arg1,Thbs1,Clec4n,Cxcl3,Ccl7 Down: Rnase6,Ear2
DC	25	Cell chemotaxis/Positive regulation of defense response	Up: Ifitm1,Ccr7,Fabp5,Pfkp,Ccl22 Down: Rpl9-ps6,Clec4b1,Cd209a,Mgl2,Tnip3
Lymphocyte	26	Leukocyte apoptotic process/Metalloprotease DUBs	Up: Ccl5,Dusp2,Ccl3,Gzma,Lck Down: H2-Aa,Lyz2,Cd74,Ly6d,Xcl1
FB	14	Myoblast differentiation/Structural constituent of ribosome	Up: Angptl4,Ccl4 Down: Dbp,Ifi27l2a,Nme2

DEGs listed as up displayed increased expression in MCAO and DEGs listed as down showed decreased expression in MCAO compared with Sham. The gene enrichment analysis was performed based on ontology sources including KEGG Pathway, GO Biological Processes, Molecular Function and Reactome Gene Sets. P-values were adjusted using the Benjamini-Hochberg correction for multiple tests.

Table S3. Top 50 differentially expressed genes per cluster among all detected brain cells.

EC	MG	ASC	EPC	SMC	MdC	CAM	OLG	PC	NEUT	FB	LYM	CPC	NPC
Foxq1	P2ry12	Ntm	Cox8b	Tagln	Arg1	Lyve1	Kcna1	Ccl11	Retnlg	Scgb1c1	Xcl1	Plvap	Npy
Abcb1a	Gpr34	Cldn10	Sostdc1	Pln	Chil3	Mrc1	Plp1	Il11	Gm5483	Inmt	Gzmb	Plpp1	Fabp7
Slco1a4	Siglech	Btbd17	Calml4	Map3k7cl	Sirpb1c	Ms4a7	Mog	Kcnj8	Il1f9	Lum	Gzma	Igfbp3	Ptn
Gm694	Hexb	Aldoc	Ttr	Acta2	Plac8	Pf4	Ermn	Ccl19	S100a9	Dcn	Cd3g	Rgcc	Apod
Itm2a	Tmem119	Nkain4	Folr1	Lmod1	Ly6c2	F13a1	Opalin	Atp13a5	Mmp9	Coch	Nkg7	Rbp7	Ccnd2
Sox17	Olfml3	Mmd2	Kcnj13	Cnn1	Ccr2	Saa3	Cldn11	Art3	Wfdc21	Col1a1	Cd3d	Nrp1	Ncam1
Cldn5	Gpr84	Scg3	1500015O10Rik	Myh11	Ms4a4c	Gpx3	Stmn4	Vtn	S100a8	Wfdc18	Ptprcap	Cd24a	Sox11
Degs2	Crybb1	Acsbg1	Pcp4	Tpm2	AA467197	Mgl2	Nkx6-2	P2ry14	Hba-a1	Slc6a13	Ly6d	Cd300lg	Nnat
Scgb3a1	Lag3	Aqp4	Hemk1	Myl9	S100a4	Apoe	Tmem151a	Higd1b	Hbb-bt	Efemp1	Ms4a4b	Gpihbp1	Tubb3
Sdpr	Ly86	Timp4	Enpp2	Aspn	Thbs1	Ccl7	Hapln2	Meg3	Hba-a2	Islr	Ccl5	Thrsp	Gsn
Ocln	Selplg	Gpr37l1	Ppp1r1b	Des	Clec4e	Maf	Mag	Il34	Mmp8	Nov	Klrk1	Slc43a3	Frzb
Tmem252	Lpcat2	Gjb6	Spint2	Mylk	Ccl6	Clec4n	Gjb1	Slc6a20a	Hbb-bs	Col1a2	Ltb	Plpp3	Stmn1
Vwa1	Cx3cr1	Fabp7	Rdh5	Sncg	Lyz2	Lyz2	Aspa	Cox4i2	Cxcr2	Igfbp5	Klrd1	Emcn	Rtn1
Flt1	Trem2	Agt	Chchd10	Mustn1	Mcemp1	Stab1	Pex5l	Sod3	Ltf	Serpinf1	Gimap4	Fam167b	Hmgn2
Ly6c1	Ccl4	Hes5	Igfbp2	Crispld2	Clec4n	Ms4a6c	Sez6l2	Ndufa4l2	G0s2	Igfbp6	Sept1	Prss23	Igfbpl1
Emcn	Ptgs1	Cxcl14	Slc22a17	Gm13861	Cfp	Ms4a6b	Mobp	Pdgfrb	Ngp	Mgp	Hcst	Timp3	Meg3
Kank3	Lpl	Cspg5	Rbp1	Rgs4	Clec4d	Lst1	Klk6	Rgs5	Hdc	Serping1	AW112010	Ramp3	Lmo4
Adgrl4	Syngr1	Ntsr2	Fxyd1	Filip1l	Napsa	Dab2	Tmeff2	Gper1	Camp	Pcolce	H2-Q7	Plscr2	Hist1h2ap
Cxcl12	Fcrls	F3	Pcolce	Crip1	Hp	Ifi27l2a	Epb41l3	Lhfp	Slpi	Gsn	Dusp2	Cd200	Pfn2
Paqr5	Lair1	Pantr1	Mcee	Cald1	Camp	Adgre1	Tnfaip6	Fstl1	Fpr1	Apod	H2-DMb2	AW112010	Gpm6b
Ctla2a	Ccl3	Lcat	Gpx8	Gm13889	Slfn1	Fcgr2b	Olig1	Slc19a1	Il1r2	Slc6a20a	Rac2	Mfap2	Apoe
Abcg2	Csf1r	Lsamp	Mdh1	Perp	Cxcl3	H2-Eb1	Gpr37	Nbl1	Ifitm6	Nupr1	Hist1h2ap	Plscr1	Meis2
Ly6a	Ccl12	Gria2	Ldhb	Gja4	Ngp	Hmox1	Cnp	Ifitm1	Trem1	Vtn	Lsp1	Clec14a	Mdk
Pecam1	Rgs10	Mlc1	Ifi27	Map1b	Ifitm6	Ms4a6d	Mbp	Ednrb	Wfdc17	Bgn	Cd52	Col13a1	S100b
Egfl7	C1qc	Scrg1	Atp5g1	Tpm1	Tgfbi	Fpr1	Tubb3	Rgs4	Cxcl3	Il34	Hmgb2	Iigp1	Dlx2
Ramp2	C1qb	Ptprz1	Atp1b1	Ndufa4l2	S100a6	Tgfbi	Aplp1	Bgn	Il1b	Timp1	S100a10	Esm1	Plp1
Ptprb	Lgmn	Dclk1	Mt3	Flna	Plbd1	Ccr1	Tubb4a	Timp1	Hp	Slc7a11	Ly6c2	Car8	Tubb2b

Pglyrp1	Mafb	Slc1a2	Ndufa1	Gper1	Slpi	Cd74	Ptgds	Gm13889	Cxcl2	Igfbp4	S100a4	Gngt2	Matn4
Mpzl1	C1qa	Ttyh1	Dbi	Rgs5	Il1b	Gmfg	Mapt	Cald1	Mxd1	Fstl1	Gmfg	Igfbp7	Tuba1a
Slc2a1	Ctss	Bcan	Ndufa11	Serping1	Cxcl2	Snx2	Tspan2	Rarres2	Chil1	Slc38a2	Lgals1	Tm4sf1	Fxyd6
Adgrf5	C3ar1	Slc1a3	Usmg5	Bgn	Osm	Cfp	Il33	Gja4	Anxa1	Nbl1	Coro1a	Meox1	Stmn2
Lsr	Bin2	Gm3764	Pebp1	Nbl1	Lgals3	Ptpn18	Phactr3	Slc6a13	Clec4e	F3	Ptpn18	Mgll	6330403K07Rik
Sgms1	Vsir	Gpm6a	Ndufv3	Csrp1	Trem1	Lgals1	Kctd13	Gm13861	Mcemp1	Igfbp2	Cd74	Ifitm2	Fxyd1
Wfdc1	Rgs1	Htra1	2010107E04Rik	Fstl1	Ccr1	Marcksl1	Dbndd2	Sdc2	Slfn1	Ptgds	Limd2	Jam3	Brinp3
Slc22a8	Abi3	Tspan7	Cox7b	Lhfp	S100a10	H2-Aa	Etv1	Gpx8	Ltb	Rbp1	Arhgdib	Mmrn2	Sox4
Slc7a5	Irf8	Gfap	Uqcr10	Cox4i2	Cd52	H2-Ab1	Fez1	Phlda1	Clec4d	Cp	Ccr2	Tgtp2	Scrg1
Car4	Cd14	Plpp3	Hist1h2bc	Higd1b	Wfdc17	Ctsc	Gpd1	Dcn	Ifitm1	Itih5	H2-Eb1	Gimap4	Slc4a4
Slc9a3r2	Sirpa	Fbxo2	Rarres2	Errfi1	Lsp1	Pla2g7	Pcdh9	Ptn	Lcn2	Ccl19	H2-Aa	Mfge8	Qpct
Esam	Aif1	Kcnk1	Fam213a	Ppp1r14a	Bcl2a1d	Ccl9	Tmod2	Lum	Msrb1	Ptn	S100a6	Lmcd1	Marcksl1
Acvrl1	Cd68	Ntrk2	Arl6ip1	Pdgfa	Ltf	Cited2	Trf	Serping1	Cd24a	Lmo4	Ccnd2	Tgtp1	Dlx1
Spock2	Fcgr3	Tubb2b	Cox6c	Sdc2	Anxa1	Fcer1g	Gpm6b	Perp	Ccrl2	Plpp3	Cd209a	Exoc3l2	Sp9
Ablim1	Rgs2	Slc6a1	Gpx4	Il34	Ms4a6c	Ccl2	Cmtm5	G0s2	Ccr1	Gpx8	Tmsb10	Mndal	Dbi
Cd200	Ctsd	Gja1	Hint2	Pdgfrb	Msrb1	Wfdc17	Cryab	Aspn	Slc7a11	Tmeff2	Napsa	Tspan15	Cmtm5
Gimap6	Cst3	Acsl3	Cox8a	Mob2	Pim1	Pid1	Cpox	Col1a2	S100a11	Lhfp	H2-Ab1	Igtp	Mgst1
Id1	Marcks	Slc7a10	Ndufa4	Actn1	Ifi27l2a	Ccl6	Tppp3	Atp1a2	Rac2	Cd302	Hn1	Gm12216	Map1b
Tsc22d1	Abhd12	Atp1b2	Ndufc1	Ppp1r12a	Ccl9	Aif1	Qdpr	Sept4	Gmfg	Lrp1	Lcp1	Col4a1	Nrxn3
Eng	Laptm5	Clu	Uqcr11	Dstn	Lst1	Ednrb	Shisa4	Col1a1	S100a6	Perp	Shisa5	Ces2e	Tmod2
Igf1r	Ltc4s	Thrsp	Slc6a20a	Ptrf	Gsr	C1qa	Sept4	Cp	Il1rn	Atp1a2	Rps27	Ifi203	Tiam2
Bsg	C5ar1	Hepacam	Atp5g3	Ptp4a3	Pid1	Clec4d	Syt11	Adap2os	Hcst	Phlda1	Rpsa	Tnfaip2	Hsph1
Cd34	Unc93b1	Gstm5	Kcnk1	Slc19a1	Emp3	Hcst	Desi1	Eva1b	Lrg1	Gjb6	Rps15a	Lrg1	Gm17750